

# Integration of plasmonic trapping in a microfluidic environment

Lina Huang,<sup>1</sup> Sebastian J. Maerkl<sup>2</sup> and Olivier J. F. Martin<sup>1</sup>

<sup>1</sup> Nanophotonics and Metrology Laboratory,  
Swiss Federal Institute of Technology Lausanne, Switzerland

<sup>2</sup> Laboratory of Biological Network Characterization,  
Swiss Federal Institute of Technology Lausanne, Switzerland

[lina.huang@epfl.ch](mailto:lina.huang@epfl.ch)

<http://nam.epfl.ch>

**Abstract:** Near field generated by plasmonic structures has recently been proposed to trap small objects. We report the first integration of plasmonic trapping with microfluidics for lab-on-a-chip applications. A three-layer plasmo-microfluidic chip is used to demonstrate the trapping of polystyrene spheres and yeast cells. This technique enables cell immobilization without the complex optics required for conventional optical tweezers. The benefits of such devices are optical simplicity, low power consumption and compactness; they have great potential for implementing novel functionalities for advanced manipulations and analytics in lab-on-a-chip applications.

© 2009 Optical Society of America

**OCIS codes:** (240.6680) Surface plasmon; (020.7010) Trapping; (350.4855) Optical manipulation.

## References and links

1. A. Ashkin, "Acceleration and trapping of particles by radiation pressure," *Phys. Rev. Lett.* **24**, 156–159 (1970).
2. A. Ashkin and J. M. Dziedzic, "Optical trapping and manipulation of viruses and bacteria," *Science* **235**, 1517–1520 (1987).
3. S. M. Block, L. S. B. Goldstein, and B. J. Schnapp, "Bead movement by single kinesin molecules studied with optical tweezers," *Nature* **348**, 348–352 (1990).
4. M. Zahn and S. Seeger, "Optical tweezers in pharmacology," *Cell. Mol. Biol.* **44**, 747–761 (1998).
5. T. N. Buican, M. J. Smyth, H. A. Crissman, G. C. Salzman, C. C. Stewart, and J. C. Martin, "Automated single-cell manipulation and sorting by light trapping," *Appl. Opt.* **26**, 5311–5316 (1987).
6. C. Bustamante, Z. Bryant, and S. B. Smith, "Ten years of tension: single-molecule DNA mechanics," *Nature* **421**, 423–427 (1987).
7. A. H. Barnett, S. P. Smith, M. Olshanii, K. S. Johnson, A. W. Adams, and M. Pretiss, "Substrate-based atom waveguide using guided two-color evanescent light fields," *Phys. Rev. A* **61**, 023608 (2000).
8. F. L. Kien, V. I. Balykin, and K. Hakuta, "Atom trap and waveguide using a two-color evanescent light field around a subwavelength-diameter optical fiber," *Phys. Rev. A* **70**, 063403 (2004).
9. S. Kuriakose, D. Morrish, X. Gan, J. W. M. Chon, K. Dholakia, and M. Gu, "Near-field optical trapping with an ultrashort pulsed laser beam," *Appl. Phys. Lett.* **92**, 081108 (2008).
10. S. Kawata and T. Sugiura, "Movement of micrometer-sized particles in the evanescent field of a laser beam," *Opt. Lett.* **17**, 772–774 (1992).
11. S. Kawata and T. Tani, "Optically driven Mie particles in an evanescent field along a channeled wave guide," *Opt. Lett.* **21**, 1768–1770 (1996).
12. L. N. Ng, M. N. Zervas, J. S. Wilkinson, and B. J. Luff, "Manipulation of colloidal gold nanoparticles in the evanescent field of a channel waveguide," *Appl. Phys. Lett.* **19**, 1439–1444 (2000).
13. K. Grujic and O. G. Helleso, "Sorting of polystyrene microspheres using a Y-branched optical waveguide," *Opt. Express* **13**, 1–7 (2004).

14. M. Kerker and C. G. Blatchford, "Elastic scattering, absorption, and surface-enhanced Raman scattering by concentric spheres comprised of a metallic and a dielectric region," *Phys. Rev. B* **26**, 4052–4063 (1982).
15. K. Svoboda and S. M. Block, "Optical trapping of metallic Rayleigh particles," *Opt. Lett.* **19**, 930–932 (1994).
16. T. Sugiura and T. Okada, "Gold-bead scanning near-field optical microscope with laser-force position control," *Opt. Lett.* **22**, 1663–1665 (1997).
17. H. Furukawa and I. Yamaguchi, "Optical trapping of metallic particles by a fixed Gaussian beam," *Opt. Lett.* **23**, 216–218 (1998).
18. P. C. Ke and M. Gu, "Characterization of trapping force on metallic Mie particles," *Appl. Opt.* **36**, 1439–1444 (1999).
19. R. Quidant, D. Petrov, and G. Badenes, "Radiation forces on a Rayleigh dielectric sphere in a patterned optical near field," *Opt. Lett.* **30**, 1009–1011 (2005).
20. G. Volpe, R. Quidant, G. Badenes, and D. Petrov, "Surface plasmon radiation forces," *Phys. Rev. Lett.* **96**, 238101 (2006).
21. M. Righini, A. S. Zelenina, C. Girard, and R. Quidant, "Parallel and selective trapping in a patterned plasmonic landscape," *Nature Phys.* **3**, 477–480 (2007).
22. X. Miao and L. Y. Lin, "Trapping and manipulation of biological particles through a plasmonic platform," *IEEE J. Sel. Top. Quantum Electron.* **13**, 1655–1662 (2007).
23. A. N. Grigorenko, N. W. Roberts, M. R. Dickinson, and Y. Zhang, "Nanometric optical tweezers based on nanostructured substrates," *Nature Photon.* **2**, 365–370 (2008).
24. M. Righini, P. Ghenuche, S. Cherukulappurath, V. Myroshnychenko, F. J. Garcia de Abajo, and R. Quidant, "Nano-optical trapping of Rayleigh particles and Escherichia coli bacteria with resonant optical antennas," *Nano Lett., Articles ASAP*, (2009).
25. L. Huang and O. J. F. Martin, "Reversal of the optical force in a plasmonic trap," *Opt. Lett.* **33**, 3001–3003 (2008).
26. P. C. Chaumet, A. Rahmani, and M. Nieto-Vesperinas, "Local-field enhancement in an optical force metallic nanotrap: application to single-molecule spectroscopy," *Appl. Opt.* **45**, 5185–5190 (2006).
27. K. Halterman, J. M. Elson, and S. Singh, "Plasmonic resonances and electromagnetic forces between coupled silver nanowires," *Phys. Rev. B* **72**, 075429 (2005).
28. B. Sepulveda, J. Alegret, and M. Käll, "Nanometric control of the distance between plasmonic nanoparticles using optical forces," *Opt. Express* **15**, 14914–14920 (2007).
29. E. Lamothe, G. Lévêque, and O. J. F. Martin, "Optical forces in coupled plasmonic nanosystems: Near field and far field interaction regimes," *Opt. Express* **15**, 9631–9644 (2007).
30. A. S. Zelenina, R. Quidant, and M. Nieto-Vesperinas, "Enhanced optical forces between coupled resonant metal nanoparticles," *Opt. Lett.* **32**, 1156–1158 (2007).
31. O. J. F. Martin and N. B. Piller, "Electromagnetic scattering in polarizable backgrounds," *Phys. Rev. E* **58**, 3909–3915 (1998).
32. M. Paulus and O. J. F. Martin, "Light propagation and scattering in stratified media: a Green's tensor approach," *J. Opt. Soc. Am. A* **18**, 3909–3915 (2001).
33. P. B. Johnson and R. W. Christy, "Optical constants of the noble metals," *Phys. Rev. B* **6**, 4370–4379 (1972).
34. M. A. Unger, H. P. Chou, T. Thorsen, A. Scherer, and S. R. Quake, "Monolithic microfabricated valves and pumps by multilayer soft lithography," *Science* **288**, 113–116 (2000).
35. T. Thorsen, S. J. Maerkl, and S. R. Quake, "Microfluidic large-scale integration," *Science* **298**, 580–584 (2002).
36. B. Lukic, S. Jeney, C. Tischer, A. J. Kulik, L. Forro, and E.-L. Florin, "Direct observation of nondiffusive motion of a Brownian particle," *Phys. Rev. Lett.* **95**, 160601 (2005).
37. B. Lukic, S. Jeney, Z. Sviben, A. J. Kulik, E.-L. Florin, and L. Forro, "Motion of a colloidal particle in an optical trap," *Phys. Rev. E* **76**, 011112 (2007).
38. V. R. Daria, P. J. Rodrigo, and J. Glckstad, "Dynamic formation of optically trapped microstructure arrays for biosensor applications," *Biosens. Bioelectron.* **19**, 1439–1444 (2004).
39. D. D. Carlo, N. Aghdam, and L. P. Lee, "Single-cell enzyme concentrations, kinetics, and inhibition analysis using high-density hydrodynamic cell isolation arrays," *Anal. Chem.* **78**, 4925–4930 (2006).

## 1. Introduction

Optical tweezers were first proposed by Ashkin and his collaborators in 1970 [1]. Small objects are trapped in the middle of a tightly focused laser beam by the optical field gradient. In 1987 Ashkin reported the first manipulation of viruses and bacteria in a single laser gradient trap created with an Argon laser [2]. This technique, which offers a damage-free method for cell manipulation, has become extremely widespread in biology for example to study kinesin molecular movement [3], for drug screening [4], cell sorting [5], investigating DNA mechanics [6] and so on.

While conventional tweezers rely on far field interactions, a new class of trapping experiments based on the near field has emerged over the last few years. In these experiments, the near field was generated in the form of an evanescent wave at the interface between two different media. The near field has been used to trap atoms [7–9] and to guide particles [10–13].

More recently, plasmonic nanostructures have entered the field of optical trapping, either as trapped particles or as trapping structures. Plasmon resonances represent resonant excitation of the free electrons in a metal and manifest either as localized modes in particles or delocalized modes in thin films [14]; they can occur in the visible or near-infrared spectrum range in metals such as gold, silver, copper and aluminum. Since these modes produce very strong and localized electromagnetic fields, they have the potential of creating even stronger trapping potentials than a tightly focused laser beam. Furthermore, since the polarizability of plasmonic particles is extremely large, they can be easily trapped in a conventional optical tweezer. The latter effect has been studied in detail by several groups [15–18]. On the other hand, the direct utilization of plasmonic nanostructures to trap dielectric or biological species has been demonstrated by a few groups [19–24]. Finally, the combination of both techniques, i.e. the utilization of a plasmonic nanostructure to generate the trap and a plasmonic particle as trapped particle opens additional degrees of freedom related to the plasmonic properties of both systems [25]. The interaction mechanisms between a pair of plasmonic particles have also been studied by several groups [26–30].

Compared to a conventional optical tweezer, trapping based on plasmonic nanostructures provides a significant improvement in that it does not require complicated optics to create the trap, which instead is simply generated by the near field of the plasmonic nanostructure. For this reason, plasmonic trapping can be easily integrated with microfluidics for lab-on-a-chip applications in order to produce novel chips with increased functionalities.

In this paper, we demonstrate such an integrated device and show for the first time how plasmonic nanostructures integrated in a microfluidic chip can be used to trap different types of dielectric structures, including living cells. The paper is organized in the following manner: in Sec. 2 we investigate numerically how a gold nanostructure can create a stable trap for a dielectric sphere; Sec. 3 describes the integration of this plasmonic structure into microfluidics; Sec. 4 demonstrates experimentally the trapping of dielectric spheres and yeast cells flowing into the microfluidic channel. A conclusion is given in Sec. 5.

## 2. Simulations

In order to gain insights into the trapping mechanisms associated with plasmonic nanostructures, we first compute the trapping potential created by a plasmonic nanostructure using the Green's tensor technique [31, 32]. The plasmonic structure is a gold disk with diameter 100 nm and thickness 40 nm (the data from Ref. [33] are used for the permittivity of the metal). For the trapped object, we first consider a dielectric sphere with diameter 10 nm and permittivity 2.25. The gold nanostructure is deposited on a dielectric substrate (permittivity 2.25) and illuminated with a planewave propagating along the  $y$ -direction under total internal reflection (incident angle  $70^\circ$ ), as shown in Fig. 1(a).

Figure 1(b) shows the field distribution in an  $xy$ -plane 10 nm above the disk at the resonant illumination wavelength  $\lambda = 608$  nm; the white circle represents the edge of the plasmonic nanostructure and serves as guide for the eye. A strong field enhancement at the edge of the disk, along the propagation direction of the illumination field can be observed. This highly localized field produces strong field gradients which generate a large trapping potential, as illustrated in Fig. 1(c). This panel shows the vertical component ( $z$ -component) of the optical force in the observation plane. The optical force is computed from the electromagnetic field distribution using the dipolar approximation [26]. Figure 1(d) shows the transverse components

( $xy$ -components) of the optical force; they push the particle toward the center of the trap. Thus, the simulations indicate that these three components create a stable optical trap for the dielectric sphere.

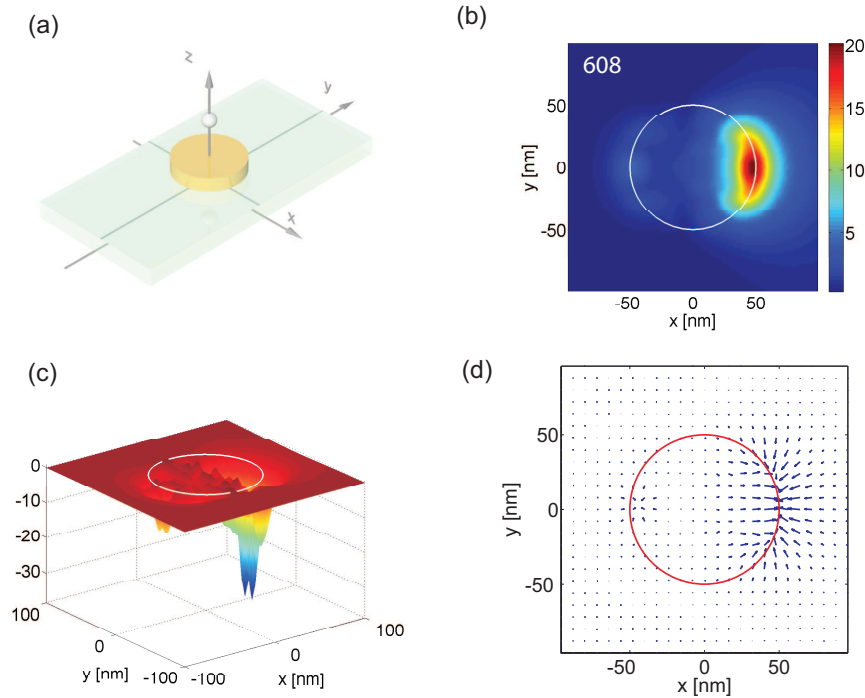


Fig. 1. (a) Simulation model: a gold disk is deposited on a glass substrate ( $\epsilon = 2.25$ ) and is illuminated at the plasmon resonance wavelength. The propagation vector is in the  $xz$ -plane and incident under total internal reflection. The incident field is polarized in the  $xz$ -plane. A dielectric sphere is used to examine the trapping force. (b) Near field intensity distribution map 10nm above the gold disk. Computed optical force in a plane 10nm above the gold nanostructure: (c)  $z$ -component and (d)  $xy$ -component.

### 3. Optofluidic integration

Compared to conventional optical tweezers, plasmonic trapping does not require complex far field optics to create the trapping potential. The latter is simply generated by the near field associated with the plasmonic nanostructure. Hence the illumination used in the experiment is quite simple, as shown in Fig. 2: a classical Kretschmann configuration is used where the optofluidic device is attached to the prism surface with an index matching gel (Thorlabs, G608N). The infrared ( $\lambda = 810\text{nm}$ ) laser light is coupled using an optical fibre into the system and excites the plasmon resonances of the gold disks. The illumination intensity on the substrate is estimated to be  $10^{-2}\text{mW}/\mu\text{m}^2$ , which is much smaller than that used in Ref. [23]. This setup is realized beneath a dark field optical microscope (Nikon OPTIPHOT 150) to observe the trapping phenomenon in reflection using white light illumination and cutting off the trapping wavelength with a filter.

The microfluidic chip is made from PDMS (Silicone elastomer polydimethylsiloxane, Dow Corning GmbH) using the process of multilayer soft lithography [34, 35]. A relatively simple

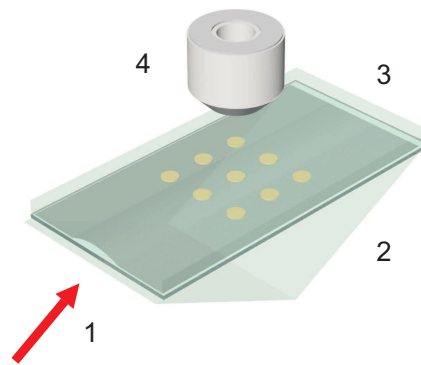


Fig. 2. Sketch of the experiment: 1: laser, 2: prism, 3: microfluidic chip, 4: dark field objective. The Plasmonic lab-on-a-chip is attached on a prism with an index matching gel. The external field is coupled into the chip through total internal reflection; incident illumination wavelength:  $\lambda = 810\text{nm}$ .

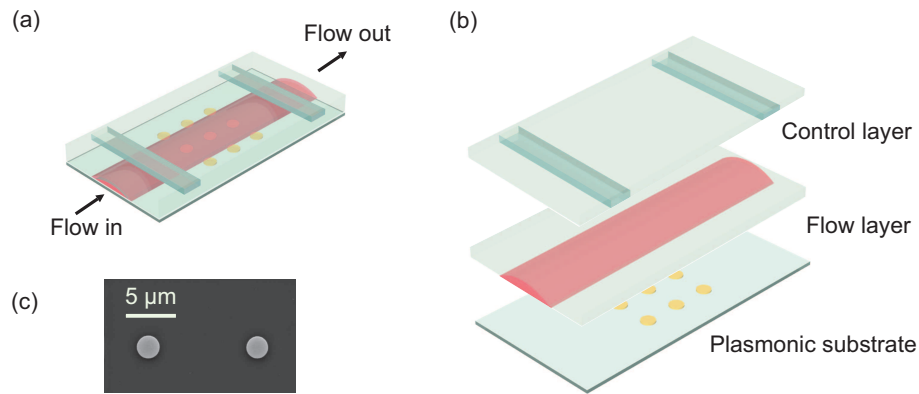


Fig. 3. Optofluidic lab-on-a-chip: (a) general view; (b) exploded view. The chip is made of three layers: the plasmonic substrate, the flow layer, and the control layer. (c) SEM image of the fabricated gold plasmonic structures on the dielectric substrate; scale bar  $5\mu\text{m}$ .

design is used here since the main functional requirement is control of the fluid speed across the plasmonic trapping structures. This chip consists of three layers, as indicated in Fig. 3. The bottom layer represents the plasmonic substrate which includes metallic nanostructures fabricated with conventional photolithography and lift-off. Two disk diameters are investigated:  $2\mu\text{m}$  and  $3\mu\text{m}$ , requiring illumination at  $\lambda = 810\text{nm}$ . The  $40\text{nm}$ -thick metal is deposited using Joule effect and includes a  $3\text{nm}$  thick chromium adhesion layer on the glass substrate. The quality of this substrate is checked using scanning electron microscope, as shown in Fig. 3(c).

The intermediate flow layer is a thin PDMS layer (thickness approximately  $100\mu\text{m}$ ) with embedded flow channels. The channel has a vaulted cross section with a maximum height of  $15\mu\text{m}$  and a width of  $150\mu\text{m}$ .

The control layer is also made of PDMS, with a thickness of approximately  $3\text{mm}$ . Control channels are embedded in the bottom of this layer and run in the directions normal to the flow channels. The control channels have a rectangular cross section (height  $20\mu\text{m}$  and width

150  $\mu\text{m}$ ). By controlling the pressure in the control channels, one can slow down or even stop the liquid flowing in the flow channels. Those control channels work as micro valves and allow for an accurate control of the flow speed. Closing these micro valves reduces the flow speed considerably, so that particles flowing in the channel can be trapped at the vicinity of the plasmonic nanostructures. Opening the micro valves allows to flush away the trapped specimen.

#### 4. Results and discussion

Commercially available 2  $\mu\text{m}$  and 3  $\mu\text{m}$  diameter polystyrene spheres (Polysciences Inc.) are first used in the experiment. The spheres are suspended in deionized water and, to prevent aggregation, are sonicated in an ultrasonic bath for 20 minutes before the experiment. Figure 4(a) ([Media 1](#)) shows that they are trapped by 2  $\mu\text{m}$  sized gold disks. The first frame of this movie is shown in Fig. 4(a). The regularly positioned structures are the plasmonic traps, while the randomly distributed particles are polystyrene spheres. Some of the gold disks appear very bright: these are the structures where spheres have already been trapped. The green rectangle in Fig. 4(a) indicates the main illumination region, which means that strong plasmonic traps are mainly excited on the disks located inside this region. Gold disks located in the rest of the image produce much weaker traps. The red circle in Fig. 4(a) indicates an area where passing spheres are trapped in the movie. Notice that the smaller spheres are much more easily trapped than the large ones, illustrating the selectivity of plasmonic trapping [21]. As mentioned, the flow channel has a vaulted cross section; therefore its side walls appear as two out-of-focus horizontal lines in all the recorded images.

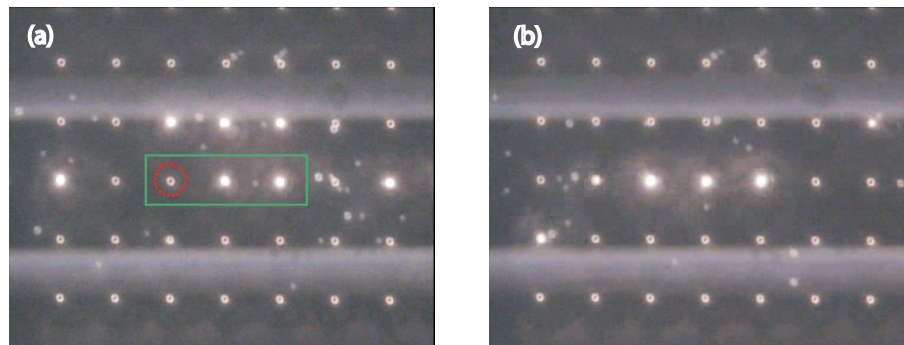


Fig. 4. (a) ([Media 1](#)) Optical plasmonic trapping of dielectric spheres in a microfluidic chip (objective 20 $\times$ ). The bright structures represent the gold disks with trapped dielectric spheres on top of them. During the movie, dielectric spheres get trapped when passing close enough to the trapping potential created by the plasmonic structures. In the highlighted red circle, small spheres appear to be much easily trapped than large ones. (b) ([Media 2](#)) Demonstration of specimen flushing using the micro valves.

In Fig. 4(a) ([Media 1](#)), the polystyrene spheres flow quite slowly from right to left in the channel since the flow is controlled by the micro valves. The spheres appear almost transparent when they are not trapped. When they pass close enough to the plasmonic gold disks, they become trapped, which makes them appear as bright spots. We believe that the spheres do not stick firmly on the gold surface since their Brownian motion is still visible [36, 37]. Trapped spheres can be easily flushed away by opening the micro valves, as shown in Fig. 4(b) ([Media 2](#)) of which the first frame is shown in Fig. 4(b). Here, the micro valves are first slightly opened causing the trapped spheres start to escape the disks. Once the valves open completely, the particles are flushed away rapidly and a new batch of particles can then be introduced and the



experiment restarted.

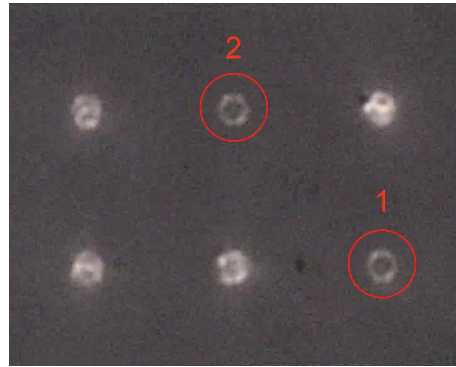


Fig. 5. ([Media 3](#)) Optical plasmonic trapping of yeast cells in a microfluidic channel (objective 50 $\times$ ). The bright structures represent the gold disks with trapped yeast cells on top of them. During the movie, a free yeast cell becomes trapped in the bottom right highlighted structure and another cell is trapped by the top highlighted disk about half a minute later.

Plasmonic trapping integrated with a microfluidic environment has the potential to become a useful tool in biology. To show the potential of plasmonic traps to manipulate biological matter, we performed an experiment with living cells. Although living cells have similar optical properties than dielectric spheres [38], trapping them optically in a microfluidic experiment remains a challenge [39]. We choose *S.cerevisiae* as it is one of the dominant model organisms in use today. Typical budding yeast cells are a few microns large. Figure 5 ([Media 3](#)) shows that yeast cells can easily be trapped in our experiment using 3  $\mu\text{m}$  diameter traps. The first frame in ([Media 3](#)) is shown in Fig. 5: the four bright disks correspond to plasmonic structures with trapped yeast cells. The other two red circles indicate plasmonic structures where no cells have been trapped at the beginning of the movie. During the experiment, a free yeast cell becomes trapped in the bottom right highlighted structure and another cell is trapped by the top highlighted disk about half a minute later. The cells remain in the trap as long as the laser is on, or until they are flushed away.

## 5. Conclusion

We have successfully demonstrated the integration of plasmonic traps with microfluidics and used it to trap different dielectric systems, including living cells. The benefit of such a device are optical simplicity, low power consumption and compactness. Plasmonic trapping has great potential for implementing novel functionalities for advanced manipulations and analytics in lab-on-a-chip applications. Finally, the trivial optics required to activate plasmonic traps will allow implementing sophisticated optical manipulations in cheap, disposable chips for point-of-care applications.

## Acknowledgment

Funding from the Swiss National Science Foundation (SNSF) (grant 200021-113735) is gratefully acknowledged.